Fine Structure of the Low-Frequency Raman Phonon Bands of Single-Wall Carbon Nanotubes

M. N. Iliev [1], A. P. Litvinchuk

*Texas Center for Superconductivity and Department of Physics,
University of Houston, Houston, TX 77204-5932*

S. Arepalli, P. Nikolaev

*G. B. Tech./ Lockheed Martin, 2400 NASA Road One, Mail Stop C61, Houston,
TX 77058*

C. D. Scott

NASA Johnson Space Center, Houston, TX 77058-3696

Abstract

The Raman spectra of single-wall carbon nanotubes produced by a laser and arc process were studied between 5 and 500 K. The line width vs temperature dependence of the low-frequency Raman bands between 150 and 200 cm^{-1} deviates from that expected for phonon decay through a phonon-phonon scattering mechanism. The experimental results and their analysis provide convincing evidence that each of the low-frequency Raman bands is a superposition of several narrower Raman lines corresponding to tubes of nearly the same diameter. At low temperatures the width $\Delta(T) = \gamma + \Gamma(T)$ of these components is determined by mainly the temperature-independent part $\gamma \approx 2$ cm^{-1}.

1 Introduction

The Raman spectra of carbon nanotubes, in particular single-wall natotubes (SWNT), have been studied intensively, both experimentally [1–7] and theoretically [8–13]. It has been established that the Raman intensities of the high-frequency tangential (1500-1600 cm^{-1}) and low-frequency radial (140-250 cm^{-1}) modes exhibit strongly resonant behavior [3–5]. It was also found that the frequency ω_b of the zone-center in-phase radial ("breathing") mode is

[1] Corresponding author, Fax: +1-713-743-8201; e-mail: iliev@jetson.uh.edu

inversely proportional to the radius of the tube and is independent [5,13] of the chiral angle. Assuming that a SWNT sample is a mixture of achiral and chiral nanotubes of different diameters, the Raman spectrum will be a superposition of spectra of all types of tubes in the scattering volume, the relative weight being determined by their abundance and Raman cross section. The existence of several peaks in the spectra between 140 and 250 cm^{-1} therefore gives evidence of tubes with various diameters between 1.1 and 2.0 nm, in agreement with the results of transmission electron microscopy (TEM) and x-ray analysis [3,14]. The issue is whether the observed Raman peaks are simple homogeneous bands or each peak corresponds to an inhomogeneously broadened complex band consisting of several overlapping simple lines of close wave numbers (diameters). In the latter case of particular interest are the parameters of the overlapping band components and their variations with temperature, as they provide information on the properties of the individual nanotubes (phonon lifetime, dominating phonon scattering mechanism, etc.) in contrast to the complex bands where this information is obscured.

In this work we report the variations with temperature of the Raman spectra of SWNT in the temperature range between 5 K and 500 K. In particular we studied in detail the behavior of the well resolved peak near 165 cm^{-1} (at 300 K), corresponding to the radial in-phase-vibration mode of tubes of diameter close to 1.36 nm. While the temperature dependence of the line width for the latter peak is inconsistent with the expectations for an anharmonic decay of a single phonon through phonon-phonon scattering, the experimental data can satisfactorily be explained within such a mechanism by considering the 165 cm^{-1} band as a superposition of several closely lying components.

2   Samples and Experimental

The SWNT samples were obtained by arc and laser production methods. The arc method is similar to that described in Ref.[15] using a 20 cm water cooled inner cylinder located inside a 30 cm chamber. The target contained 4% Ni and 1% Co as catalysts. The run conditions were: 35 volts; 100 amp.s; 100 sccm flow of helium at 66.7 kPa (500 Torr). Part of the "collarette" deposit on the cathode was used for making a "bucky paper" (felt-like) sample for characterization. The laser method is described in Ref.[16] and is a two-laser oven method used originally by Smalley's group with 1% Ni and 1% Co catalysts. The run conditions were: green laser pulse (300 mJ, 5mm diameter) followed by IR laser pulse (300 mJ, 5 mm diameter) after 50 nsec; 5 cm quartz flow tube in an oven at 1200°C with 100 sccm argon flow at 66.7 kPa (500 Torr). The carbon soot containing the nanotubes deposited on the walls of the quartz tube was used for making bucky paper as follows. The material (10 mg) was sonicated in acetone and filtered through a teflon membrane filter (25 mm di-

2

ameter, 5 μm pore size; Mitex)under vacuum. The dried bucky paper removed from the filter paper was used for Raman characterization studies.

The Raman spectra were measured using the He-Ne laser line (632.8 nm) and a single spectrometer (1800 gr/mm grating), equipped with an optical microscope ($\times 50$ objective), a notch filter and a liquid-nitrogen-cooled charge-coupled device (CCD) detector with 15×15 μm pixel size. The spectral resolution was 1.3 cm^{-1} as evidenced by the width of the laser plasma lines. The samples (2×2 mm in size) were mounted in a Microstat^{He} cryostat (Oxford Instrument), where the temperature could be varied between 5 and 500 K. To minimize the local laser heating, the laser power in the focus spot of 5-7 μm diameter was kept below 0.5 mW, which corresponds to an averaged laser power density of 1000-2000 W.cm^{-2}. Further reduction of the laser power had no effect on the spectral line shape. The spectra taken from different spots on the surface of the same sample were practically identical, a fact which indicates the homogeneity of the samples studied.

3 Results and Discussion

Fig.1 shows the low-frequency and high-frequency parts of the Raman spectra of SWNTs as obtained at 10 K from the two samples used in our experiments, namely, Sample #1, prepared by the laser process [16] and Sample #2, prepared by the arc process [15]. As follows from Fig.1, the Raman spectra of Sample #1 and Sample #2 are very similar and exhibit well pronounced maxima at 167, 184-185, 190-192, and 195 cm^{-1} in the region of the radial A_{1g} (or A) phonon modes. They correspond to tube diameters of 1.35, 1.22, 1.17-1.18, and 1.15 nm, respectively, as estimated using the relation $\omega_b d = 223.75$ cm^{-1}nm [5]. In the high-frequency region between 1200 and 1800 cm^{-1} the spectra of Samples #1 and #2 at 10 K exhibit peaks at 1324, 1549, 1589, 1602, and 1754 cm^{-1} (at room temperature these peaks are at 1321, 1546, 1589, and 1598 cm^{-1}. Following the analysis of Kasuya et al.[2] the complex structure of the 1540-1600 cm^{-1} band can be understood by zone-folding of the graphite phonon dispersion relations. The relative intensity of the broad peak at 1324 cm^{-1} is higher for Sample #2. The origin of this peak is not well understood. Its position has been found to vary strongly with the laser excitation wavelength [1] (from 1258 cm^{-1} with 1320 nm excitation to 1347 cm^{-1} with 514.5 nm) and its appearance has tentatively been assigned to a symmetry-lowering effect, such as defects of nanotube caps, bending of the nanotube, or the presence of nanoparticles and amorphous carbon. [17] The peak at 1754 cm^{-1} has been attributed to second-order Raman processes involving combinations of radial and tangential modes. [7]

Further we will concentrate on the variations with temperature of the low-

frequency part of the spectra as illustrated on Fig.2 for Sample #2. The spectra of Sample #1 vary in a similar way. The spectral line shapes of Fig.2 can be fitted by five Lorentzians and an even better fit is obtained by curves of mixed Lorentzian-Gaussian profiles. As expected, the main effect of increasing the temperature is a shift towards lower wave numbers and broadening as shown in Fig.3 for the well separated peak near 167 cm^{-1}. In the case of simple phonon lines the line width is a measure of the phonon lifetime. It is determined by the dominating scattering mechanism, which could be temperature-independent (scattering from lattice defects) or temperature-dependent (scattering from phonons). Following the standard model for anharmonic phonon decay through phonon-phonon scattering, which is valid for crystalline materials [18,19], the variations of the phonon line width with temperature $\Delta(T)$ follows the dependence:

$$\Delta(T) = \gamma + \Gamma(T) = \gamma + \Gamma_0 \left(1 + \frac{2}{e^x - 1}\right), \tag{1}$$

where γ is the temperature-independent part of the line width, $x = \hbar\omega/(2k_BT)$, $\hbar\omega$ is the phonon energy, k_B is the Boltzmann constant. Provided the 167 cm^{-1} line corresponds to a single homogenous line, one expects from Eq.(1) (for $\gamma = 0$) an increase of its width upon varying the temperature from 10 K to 500 K by factor 8.4. As it is seen from Fig.3 this is obviously not the case. This implies that a more realistic approach, which assumes contribution of several close lying homogeneous lines, is required to describe the observed temperature evolution of the band width.

We modeled the band at 167 cm^{-1} as a superposition of four close lying Lorentzian components with the maxima ω_0 at 168.1, 167.2, 164.7 and 167.5 cm^{-1}. These positions, obtained from the expression:

$$\omega_{(m,n)} = \frac{223.75}{d_{(n,m)}} = \frac{\pi 223.75}{d_{C-C}\sqrt{3}\sqrt{n^2 + m^2 + nm}} = \frac{2856}{\sqrt{n^2 + m^2 + nm}} \tag{2}$$

are the closest ones to 167 cm^{-1} and correspond to tubes of chiral indices (m,n) of (17,0), (16,2), (15,4), and (14,5), respectively. In Eqs.(2) "223.75 nm.cm^{-1}" is the experimentally determined "universal" constant [5], and $d_{C-C} = 0.142$ nm is the C-C bond length. The addition of more components at positions corresponding to other tubes of close diameter, e.g. 165.0 cm^{-1} (10,10), 164.7 cm^{-1} (11,9) and 163.9 cm^{-1} (12,8), or the replacement of any of the four components by another one at a close position does not affect significantly the results described below.

The fit of the experimental spectrum for T = 10 K was achieved by varying the intensities of the components for fixed ω_0 and given γ and Γ_0. The final resolution of the experimental setup was also taken into account by convoluting the calculated spectrum with the instrumental function. As it is seen from

Fig. 4 (lower curve), it was possible to reproduce reasonably well the experimental line shape at low temperature. Further, to estimate the temperature dependence of the linewidth, we performed a series of simulations assuming that $\Delta(T)$ of each of the components follows the dependence (1). The results of model calculations are summarized in Fig. 3 by the solid lines. As it is clearly seen, one can successfully describe the experimentally observed behavior of the band width within the whole temperature range between 0 and 500 K for $\gamma \approx 2.0$ cm^{-1} and $\Gamma_0 \approx 1.0$ cm^{-1}. Using these values and accounting for the temperature induced frequency softening by shifting all ω_0s by the same amount towards lower wave numbers, one can fit the experimental spectra at higher temperatures, as illustrated in Fig. 4 (upper curve) for T = 500 K.

The results presented above show that the Raman spectroscopy may become an efficient tool for the characterization of SWNT for tube diameter distribution. Provided the Raman cross section vs tube diameter dependence for a given laser excitation energy (wavelength) is known, the normalized experimental spectrum will represent the distribution of tubes by diameter. The normalized Raman spectrum could then be modelled as a superposition of all lines with $\omega_{(m,n)}$ within the frequency range, thus determining the relative weight of the corresponding (m,n) tubes in the sample.

4   Acknowledgments

Fig. 1. Raman spectra at 10 K of SWNT obtained by laser process (Sample #1) and arc process (Sample #2).

..

Fig. 2. Variation with temperature between 10 and 500 K of the Raman spectra in the 140-220 cm^{-1} range of Sample #2 (arc process). The spectral resolution is 1.3 cm^{-1}.
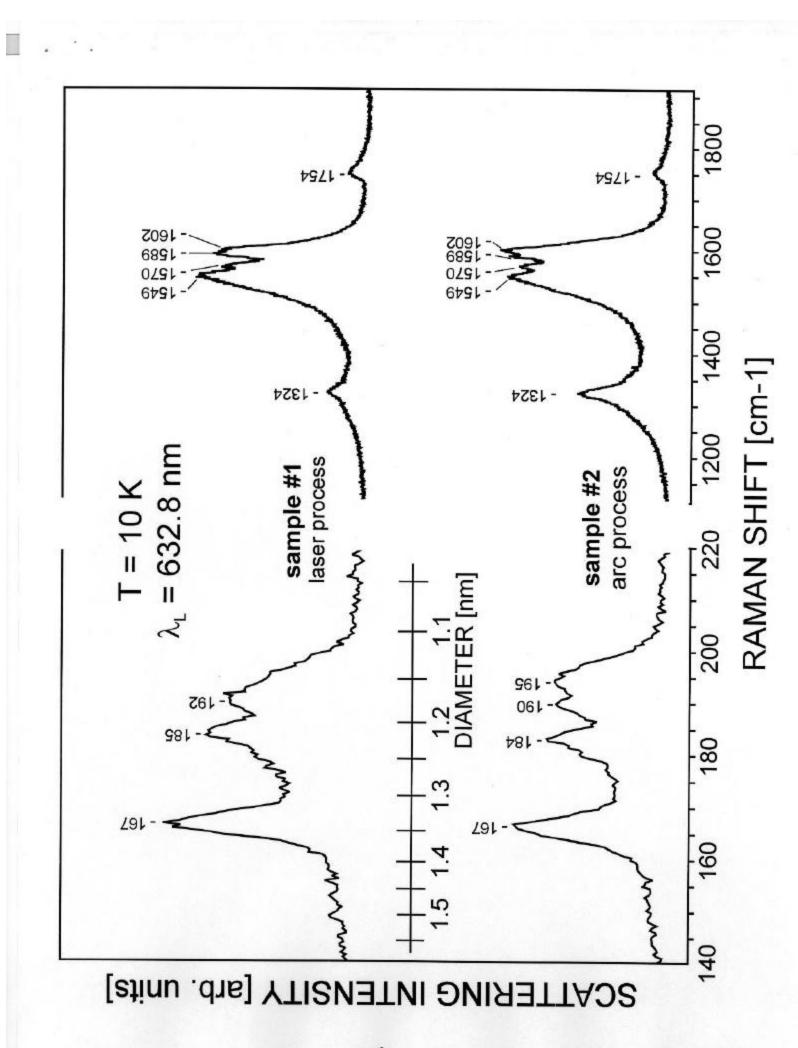
..

Fig. 3. Experimental (points) and calculated (curves) temperature dependence of the width of the 167 cm^{-1} band. The band is simulated as consisting of four close lying Lorentzian components with $\gamma = 2.0$ cm^{-1} and $\Gamma_0 = 0.5$, 1.0, and 1.5 cm^{-1}.
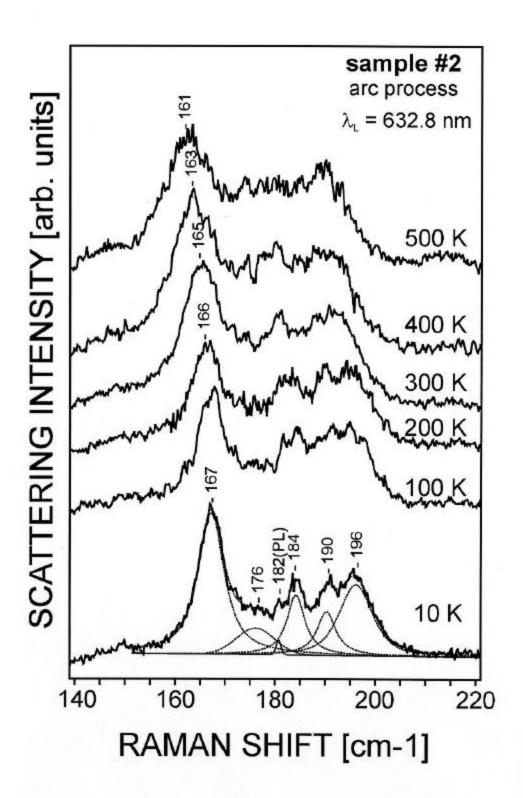
Fig. 4. Experimental (points) and calculated (curves) profiles of the 167 cm^{-1} band of Sample #2 at 10 K (lower curve) and 500 K (upper curve). The fitting parameters are $\gamma = 2.2$ cm^{-1} and $\Gamma_0 = 0.9$ cm^{-1}.
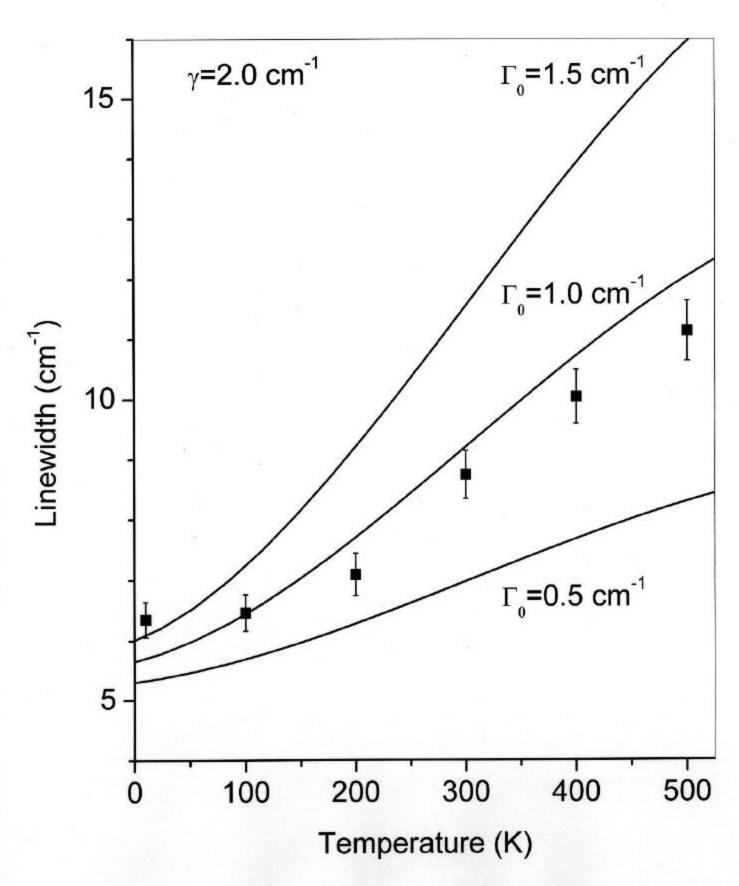
References

[1] A. M. Rao, E. Richter, S. Bandow, B. Chase, P. C. Eklund, K. A. Williams, S. Fang, K. R. Subbaswamy, M. Menon, A. Thess, R. E. Smalley, G. Dresselhaus, and M. S. Dresselhaus, Science **275** (1997) 187.

[2] A. Kasuya, Y. Sasaki, Y. Saito, K. Tohji, and Y. Nishina, Phys. Rev. Lett. **78** (1997) 4434.

[3] A. G. Rinzler, J. Liu, H. Dai, P. Nikolaev, C. B. Huffman, F. J. Rodriquez-Macias, P. J.Boul, A. H. Lu, D. Heymann, D. T. Colbert, R. S. Lee, J. E. Fischer,

A. M. Rao, P. C. Eklund, and R. E. Smalley, Appl. Phys. A **67** (1998) 29.

[4] A. Kasuya, M. Sugano, T. Maeda, Y. Saito, K. Tohji, H. Takahashi, Y. Sasaki, M. Fukushima, Y. Nishina, and C. Horie, Phys. Rev. B **57** (1998) 4999.

[5] S. Bandow, S. Asaka, Y. Saito, A. M. Rao, L. Grigorian, E. Richter, and P. C. Eklund, Phys. Rev. Lett. **80** (1998) 3779.

[6] F. Huang, K. T. Yue, P. Tan, S.-L. Zhang, Z. Shi, X. Zhou, and Zh. Gu, J. Appl. Phys. **84** (1998) 4022.

[7] M. A. Pimenta, A. Marucci, S. A. Empedocles, M. G. Bavendi, E. B. Hanlon, A. M. Rao, R. E. Smalley, G. Dresselhaus, and M. S. Dresselhaus, Phys. Rev. B **58** (1998) R16016.

[8] R. A. Jishi, L. Venkataraman, M. S. Dresselhaus, and G. Dresselhaus, Chem. Phys. Lett. **209** (1993) 77.

[9] R. Saito, T. Takeya, T. Kimura, G. Dresselhaus, and M. S. Dresselhaus, Phys. Rev. B **57** (1998) 4145.

[10] A. Charlier, E. McRae, M.-F. Charlier, A. Spire, and S. Forster, Phys. Rev. B **57** (1998) 6689.

[11] J. Kürti, G. Kresse, and H. Kuzmany, Phys. Rev. B **58** (1998) R8869.

[12] R. Saito, T. Takeya, T. Kimura, G. Dresselhaus, and M. S. Dresselhaus, Phys. Rev. B **59** (1999) 2388.

[13] V. N. Popov, V. E. Van Doren, and M. Balkanski, Phys. Rev. B **59** (1999) 8355.

[14] A. Thess, R. Lee, P. Nikolaev, H. Dai, P. Petit, J. Robert, C. Hu, Y. H. Lee, S. G. Kim, A. G. Rinzler, D. T. Colbert, G. E. Scuseria, D. Tomanek, J. E. Fischer, and R. E. Smalley, Science **273** (1996) 483.

[15] C. Journet, W. K. Maser, P. Bernier, A. Loiseau, M. Lamy de la Chapelle, S. Lefrant, P. Deniard, R. Lee, and J. E. Fisher, Nature **388** (1997) 756.

[16] S. Arepalli and C. D. Scott, Chem. Phys. Lett. **302** (1999) 139.

[17] R. Saito, G. Dresselhaus, and M. S. Dresselhaus, *"Physical Properties of Carbon Nanotubes"* (London, Imperial College Press, 1998).

[18] I. P. Ipatova, A. A. Maradudin, and R. F. Wallis, Phys. Rev. **155** (1967) 882.

[19] M. Balkanski, R. F. Wallis, and E. Haro, Phys. Rev. B **28** (1983) 1928.

SCATTERING INTENSITY [arb. units]

RAMAN SHIFT [cm-1]

sample #2
arc process
λ_L = 632.8 nm

161
163
165
166
167

176
182(PL)
184
190
196

500 K
400 K
300 K
200 K
100 K
10 K

9

M.N. Iliev at al., Fig. 3

T=500 K

T=10 K

Scattering Intensity (arb. units)

Raman shift (cm^{-1})

150   160   170

M.N. Iliev *et al.*, Fig. 4